



PHS PUBLIC ACCESS

Author manuscript

J Cardiovasc Comput Tomogr. Author manuscript; available in PMC 2015 September 22.

Published in final edited form as:

J Cardiovasc Comput Tomogr. 2015 ; 9(4): 321–328. doi:10.1016/j.jcct.2015.04.006.

Viability assessment after conventional coronary angiography using a novel cardiovascular interventional therapeutic CT system: Comparison with gross morphology in a subacute infarct swine model

Yeonggul Jang, BS^{#a}, Iksung Cho, MD^{#b}, Bríain W.Ó. Hartaigh, PhD^{c,d}, Se-Il Park, DVM, PhD^e, Youngtaek Hong, BS^a, Sanghoon Shin, MD^b, Seongmin Ha, BS^a, Byunghwan Jeon, BS^a, Hoyup Jung, PhD^f, Hackjoon Shim, PhD^g, James K. Min, MD^c, Hyuk-Jae Chang, MD, PhD^{b,g,*}, Yangsoo Jang, MD, PhD^b, and Namsik Chung, MD, PhD^{b,h}

^a Brain Korea 21 Project for Medical Science, Yonsei University, Seoul, Korea

^b Division of Cardiology, Department of Internal Medicine, Severance Cardiovascular Hospital, Yonsei University College of Medicine, 250 Seongsanno, Seodaemun-gu, Seoul 120-752, Korea

^c Department of Radiology, New York-Presbyterian Hospital and the Weill Cornell Medical College, New York, NY, USA

^d Section of Geriatrics, Department of Internal Medicine, Yale School of Medicine, Adler Geriatric Center, New Haven, CT, USA

^e Cardiovascular Product Evaluation Center, Yonsei University College of Medicine, Seoul, Korea

^f Department of Computer Science and Engineering, Hankuk University of Foreign Studies, Kyonggi, 449-791, Korea

^g Cardiovascular Research Institute, Yonsei University College of Medicine, Seoul, Korea

^h Severance Biomedical Science Institute, Yonsei University College of Medicine, Seoul, Korea

[#] These authors contributed equally to this work.

Abstract

Background—Given the lack of promptness and inevitable use of additional contrast agents, the myocardial viability imaging procedures have not been used widely for determining the need to performing revascularization.

Objective—This study is aimed to evaluate the feasibility of myocardial viability assessment, consecutively with diagnostic invasive coronary angiography (ICA) without use of additional contrast agent, using a novel hybrid system comprising ICA and multislice CT (MSCT).

Methods—In all, 14 Yucatan miniature swine models (female; age, 3 months; weight, 28–30 kg) were subjected to ICA followed by balloon occlusion (90 minutes) and reperfusion of the left anterior descending coronary artery. Two weeks after induction of myocardial infarction, delayed

* Corresponding author. hjchang@yuhs.ac (H.-J. Chang)..

Conflict of interest: The authors declare that they have no conflict of interest.

hyperenhancement (DHE) images were obtained, using a novel combined machine comprising ICA and 320-channel MSCT scanner (Aquilion ONE, Toshiba), after 2, 5, 7, 10, 15, and 20 minutes after conventional ICA. The heart was sliced in 10-mm consecutive sections in the short-axis plane and was embedded in a solution of 1% triphenyltetrazolium chloride (TTC). Infarct size was determined as TTC-negative areas as a percentage of total left ventricular area. On MSCT images, infarct size per slice was calculated by dividing the DHE area by the total slice area (%) and compared with histochemical analyses.

Results—Serial MSCT scans revealed a peak CT attenuation of the infarct area (222.5 ± 36.5 Hounsfield units) with a maximum mean difference in CT attenuation between the infarct areas and normal myocardium of at 2 minutes after contrast injection (106.4; P for difference = 0.002). Furthermore, the percentage difference of infarct size by MSCT vs histopathologic specimen was significantly lower at 2 ($8.5\% \pm 1.8\%$) and 5 minutes ($9.5\% \pm 1.9\%$) than those after 7 minutes. Direct comparisons of slice-matched DHE area by MSCT demonstrated excellent correlation with TTC-derived infarct size ($r = 0.952$; $P < .001$). Bland-Altman plots of the differences between DHE by MSCT and TTC-derived infarct measurements plotted against their means showed good agreement between the 2 methods.

Conclusion—The feasibility of myocardial viability assessment by DHE using MSCT after conventional ICA was proven in experimental models, and the optimal viability images were obtained after 2 to 5 minutes after the final intracoronary injection of contrast agent for conventional ICA.

Keywords

Multislice computed tomography; Myocardial viability; Myocardial contrast delayed; enhancement

1. Introduction

A dysfunctional myocardium can be characterized by 3 separate entities: stunning, hibernation, and scar.^{1,2} Within this spectrum, the differentiation of scar from stunning or from hibernation is essential for future prognosis, as stunning and hibernating myocardium are considered reversible with appropriate revascularization treatment.^{3–5} Various imaging modalities including stress echocardiography, single-photon emission CT, positron emission tomography, and magnetic resonance imaging (MRI) have been used to discriminate viable and nonviable myocardium.^{6,7} Of these modalities, delayed hyperenhancement (DHE) imaging using MRI has been proven to be the most reliable in the detection of myocardial scar.^{8–11} Given iodine-based contrast has similar kinetics to that based on gadolinium,¹² there has been some attempt in using multislice CT (MSCT) for DHE imaging.^{13,14} Furthermore, MSCT has demonstrated excellent correlation with DHE of MRI and histopathologic specimens.¹⁵ However, viability imaging of the myocardium has not been used extensively for determining the need to perform revascularization—primarily because viability imaging including MSCT cannot be performed simultaneously alongside invasive coronary angiography (ICA). As such, patients typically undergo coronary revascularization as a secondary procedure several days after undergoing viability imaging, which can be

time-consuming and impractical, and the patient may also be prone to potential side effects from the use of additional intravenous contrast agents.¹⁶

Recently, Sato et al demonstrated that myocardial viability imaging using DHE by MSCT could be obtained immediately after percutaneous coronary intervention (PCI) without additional use of intravenous contrast.¹⁷ A drawback of that study, however, was that patients' cardiac MSCT scans were performed after coronary revascularization; hence, these study findings are not applicable for determining coronary revascularization. Nevertheless, these observations imply that DHE imaging by MSCT after ICA without additional contrast use may be useful in overcoming some of the current limitations surrounding viability imaging. In this investigation, we therefore studied the feasibility of myocardial viability assessment, concurrent with diagnostic ICA, for the guidance of coronary revascularization using a novel hybrid system comprising ICA and MSCT.

2. Materials and methods

2.1. Animal model preparation

The study complied with the regulations of the animal care committee of the Cardiovascular Product Evaluation Center, Yonsei University, and the National Institutes of Health publication of "The 1996 Guide for the Care and Use of Laboratory Animals."¹⁸ In all, 14 Yucatan miniature swine models (female; age, 3 months; weight, 28–30 kg) were enrolled for the present study. The pigs were initially sedated with tiletamine and zolazepam (Zoletil 50; Virbac, Carros, France) 5 mg/kg and xylazine (Rompun; Bayer Korea, Seoul, South Korea) 2 mg/kg and then intubated. Anesthesia was maintained with 1% to 1.5% isoflurane in 100% oxygen gas at a flow of 1.5 mL/minute and administered by the anesthesia machine with mechanical ventilation (Primus; Dräger, Lubeck, Germany). Adequate anesthesia was confirmed by the absence of a limb withdrawal reflex. Monitoring by limb-lead electrocardiography (ECG) was performed throughout the operation with polygraph. Before procedures, ketorolac (5 mg/kg) was administered intramuscularly to relieve pain and prevent inflammation. This protocol was used for the creation of myocardial infarction, ICA, and MSCT image acquisitions.

2.2. Creation of myocardial infarction

The experimental swine model was placed in a dorsal recumbency, and the incision site was prepared aseptically with standard Betadine (Betadine, Korea Pharma, Seoul, Korea) and alcohol scrub. Fifteen minutes before balloon occlusion, all swine received 300-mg amiodarone to lower the risk of ventricular fibrillation. After placement of a 6F introducer sheath in the right carotid artery by surgical cut down, each animal received a single dose of heparin (200 U/kg) and bretylium tosylate (2.5 mg/kg). Under fluoroscopic guidance (INFX-8000V; Toshiba), a 6F Judkins left guiding catheter (Cordis; Johnson and Johnson) was positioned in the left coronary ostium. After the intracoronary administration of nitroglycerin (200 µg), coronary angiography was determined by cine-radiography to demonstrate left anterior descending (LAD) artery patency (Fig. 1). A 3.0 × 15-mm angioplasty balloon (Medtronic) was then positioned immediately distal to the first diagonal LAD vessel and inflated to normal pressure, which was dependent on its compliance chart to

achieve vessel occlusion for a period of 90 minutes, followed by reperfusion. Animals were monitored until full recovery and then were returned to housing.

2.3. Imaging data acquisition for MSCT after conventional ICA

Two weeks after inducing myocardial infarction, ICA and MSCT were performed. Swine were anesthetized as described previously. Coronary angiography and acquisition of MSCT viability imaging were performed using a novel cardiovascular interventional therapeutic CT (CVIT-CT) system, which allowed for the acquisition of coronary angiography and MSCT consecutively (Fig. 2). Before ICA procedures, a noncontrast MSCT image was obtained for the purpose of acting as a control. For ICA procedures, a CVIT-CT system was set to coronary angiography mode. To mimic clinical ICA procedures, routine coronary angiography images for the left coronary artery were obtained in right anterior oblique caudal, right anterior oblique cranial, anterior-posterior cranial, left anterior oblique cranial, and left anterior oblique caudal views, as well as anterior-posterior caudal. A total of 24 mL (4 mL per each view) contrast agent (Iomeron 400 mg/mL; Bracco, Milan, Italy) was injected intracoronary during routine ICA. After obtaining the ICA images, the CVIT-CT system was switched to MSCT acquisition mode. MSCT images were acquired using a prospective ECG-gated 320-channel scanner (Aquilion ONE; Toshiba Medical Systems, Otawara, Japan) with the following characteristics: collimation and slice thickness, 0.5 mm; reconstruction increment, 0.3 mm; reconstruction field of view, 109 to 123 mm; reconstruction kernel, FC43; reconstruction algorithm, adaptive iterative dose reduction 3D; tube rotation time, 0.35 seconds; tube voltage, 120 kVp; current, 550 mA; and prospective ECG gating, 75% R-R interval. We assessed intracoronary-injected contrast agent kinetics by tracking signal intensity of the infarct region and remote myocardial region (adjacent left ventricular free wall and mid-ventricular septum) over a duration of 20 minutes. To explore the contrast wash-in and wash-out kinetics and determine optimal image acquisition timing for DHE after intracoronary contrast injection by time delay between contrast injection and MSCT image acquisition, all MSCT scans were performed at 2, 5, 7, 10, 15, and 20 minutes after last intracoronary contrast injection, and each image was compared with histopathologic specimens. Reconstructed images were then transferred to a commercially available workstation (Vitreia fX 6.4; Toshiba Medical Systems, Otawara, Japan) for subsequent analyses.

2.4. Histopathologic specimen preparation and interpretation

The heart was removed immediately after image acquisition for sectioning and staining. The heart was sliced in 10-mm consecutive sections in the short-axis plane. To obtain a viability staining, sliced myocardia were embedded in 1% of 2, 3, 5-triphenyltetrazolium chloride (TTC) solution (Sigma-Aldrich; St. Louis, MO) at 37° C for 15 minutes, followed by fixation in a buffered 4.5% formalin solution for 20 minutes. For histopathologic specimen analysis, all slices showing myocardial scar by TTC staining were digitally photographed for further investigation. Infarct size was defined as TTC-negative area by hand planimetry for each myocardial slice and expressed as an area ratio (%) for each section using ImageJ platform (ImageJ version 1.36b; National Institutes of Health, Bethesda, MD). The area of myocardial infarction of the histopathologic specimen was measured independently from MSCT images.

2.5. Image data analysis

For MSCT image analyses, multiplanar reconstructions of axial slices were coregistered using anatomic landmarks by an independent investigator who did not further participate in MSCT analysis (Fig. 3).^{13,19–21} Thereafter, 2 experienced readers, who were level III equivalent and/or board certified in cardiovascular CT,²² were blinded to histopathologic specimen results, analyzed the MSCT images. To quantify infarct size in each matched short-axis slice, the endocardial and epicardial contours of the left ventricle and the contours of the delayed enhancement were manually measured repeatedly. Mean values from those measurements were used for further calculations. The presence of an infarct size in an MSCT image was defined as the delayed enhancement area for each matched short-axis slice and expressed as a percentage of the area of the total left ventricular wall at each slice. The percentage difference in infarct size by MSCT compared with histopathologic specimen at each time point was defined as the difference between the infarct size in MSCT and histopathologic specimen divided by the infarct size by a histopathologic specimen.

2.6. Statistical methods

For the MSCT images, the interobserver reliability in the measurement of the infarct size was assessed by means of the intraclass correlation coefficient (2-way random, single measure).²³ The CT attenuation differences between infarct tissue and remote normal myocardium at each time point were compared using paired *t* test. The infarct size measurement errors of MSCT over time were compared using repeated measures 1-way analysis of variance with Bonferroni correction for post hoc analyses. The agreement and correlation between infarct size assessed with MSCT and histopathology were evaluated with Bland-Altman analysis and the Pearson correlation coefficient, respectively. All tests were 2-sided, and $P < .05$ was regarded as statistically significant. Statistical analyses were performed using SAS (version 9.2; SAS Institute Inc., Cary, NC).

3. Results

Among 14 swine models, 2 pigs expired because of persistent ventricular fibrillation during the creation of a myocardial infarction. Thus, multidetector CT images and histopathologic images were obtained in a total of 12 pigs.

3.1. Optimal image acquisition timing for DE imaging after CAG

As illustrated in Fig. 4, myocardial delayed scan images were obtained serially at 2, 5, 7, 10, 15, and 20 minutes. MSCT identified a peak CT attenuation of the infarct area (222.5 ± 36.5 HU) and normal myocardium (116.1 ± 45 HU; Fig. 3A and B), with a maximum mean difference in CT attenuation between the infarct areas and normal myocardium of 106.4 at 2 minutes after contrast injection (P for difference = 0.002). Contrasts were subsequently washed out and the attenuation difference between infarct and normal myocardium was decreased to 65.7 ± 23.6 HU at 5 minutes (P for difference compared with normal myocardium = 0.003). The statistical significance of differences in CT attenuation between infarct area and remote normal myocardium was observed up until 15 minutes after the last intracoronary contrast injection.

We calculated the percentage difference in infarct size by MSCT compared with histopathologic specimen at each time point between 2 and 20 minutes to investigate the accuracy of MSCT infarct measures over time (Fig. 5). Mean percentage difference in infarct size by MSCT appeared to increase with time from the last intracoronary contrast injection to the MSCT image acquisition ($P = .035$, repeated measurement analysis of variance). Compared with the mean percentage difference at 2 minutes ($8.5\% \pm 1.8\%$), the mean percentage difference at 5 minutes ($9.5\% \pm 1.9\%$) did not differ materially ($P = .580$). However, the mean percentage differences vs histopathologic specimen increased significantly from 7, 10, 15, and 20 minutes (eg, $24.1\% \pm 8.2\%$, $30.0\% \pm 13.3\%$, $25.2\% \pm 17.4\%$, and $59.9\% \pm 12.7\%$, respectively) when compared with 2-minute postintracoronary contrast injection (all $P < .05$).

3.2. Comparison of the size of hyperenhanced regions on MSCT and TTC-stained area of histopathologic specimen

On the basis of the previously mentioned study findings and also considering the feasibility in the clinical setting to allow transition time from ICA to MSCT acquisition, we used the infarct measurement result at 5 minutes to test for further agreement between MSCT and histopathologic specimens. Interobserver variability for identification of infarct size between 2 experienced readers for MSCT images was intraclass correlation coefficient = 0.93 (95% confidence interval, 0.87–0.97). Direct comparisons of reconstructed slice-matched DHE area measured by MSCT after ICA demonstrated excellent correlation with TTC-derived infarct size in histopathologic specimens ($r = 0.952$; 95% confidence interval, 0.904–0.976; $P < .001$; Fig. 6A). Finally, Bland-Altman plots of the difference between DHE by MSCT and TTC-derived infarct measurements plotted against their means (Fig. 6B) demonstrated good agreement between the 2 methods.

4. Discussion

In this experimental study involving swine models, we set out to determine the feasibility of myocardial viability assessment by ascertainment of delayed-enhancement MSCT after conventional ICA without additional contrast agent use. The major finding was that myocardial viability assessment using DHE area measured by MSCT between 2- and 5-minute duration after conventional ICA displayed excellent agreement with infarct size as measured by histochemical staining.

The importance of a viability assessment using various imaging modalities for determination of revascularization treatment is well documented.^{24,25} Given the available data, current guidelines suggest viability evaluation in patients with left ventricular dysfunction and who are known to be amenable to revascularization is appropriate.²⁶ As a surprise, however, viability imaging has not been widely used in the clinical setting. One plausible explanation for its lack of use in the clinical setting to date is that it has remained a challenge to conduct viability imaging simultaneously with ICA. Current procedures after diagnosis of obstructive coronary artery disease by ICA indicate patients should undergo the following costly and time-consuming steps: (1) being discharged from the catheterization laboratory; (2) waiting for scheduling a viability imaging test; (3) undergoing a viability test; (4)

waiting for the viability imaging results; and (5) if necessary, revisiting the catheterization laboratory to undergo a secondary revascularization procedure. Furthermore, another reason that could influence the physicians' decision to use viability imaging for determining revascularization is the additional use of contrast agent required. Indeed, contrast agents required to perform an MSCT or MRI could expose the patient to potential risks including nephrotoxicity or nephrogenic systemic fibrosis.¹⁶ Although it bears mentioning, these potential side effects are more common in patients with renal dysfunction, which is prevalent in patients who are referred for viability imaging.²⁷

Foremost, the present study demonstrates that viability assessment using a novel hybrid CVIT-CT system can likely overcome these limitations. On background of present study data, the CVIT-CT system permitted accurate viability assessment without additional contrast agent administration almost concurrent with ICA. Importantly, optimal viability images were obtained after 2 to 5 minutes after the final intracoronary injection of contrast agent for conventional ICA, which is fitting with prior intravenous injection viability studies.²⁸ Conversely, the accuracy of viability assessment after intracoronary injection diminished after 7 minutes, demonstrating that the wash-out of contrast occurred at a more rapid rate than that observed under intravenous injection.²⁸⁻³⁰ Hence, quick acquisition (ie, approximately 5 minutes duration) of DHE imaging by MSCT is an important component for the accurate assessment of myocardial viability, especially when using the method described in the present study.

Moving forward, we suggested the conceptual framework (Fig. 7) that provides a stepwise, timed approach for image acquisition and interpretation process in patients with suspected coronary artery disease and severe left ventricular dysfunction. If the patient has a coronary artery disease on ICA, the CVIT-CT system is immediately switched to MSCT acquisition mode and performs a viability scan within 5 minutes. An experienced radiologist or cardiologist will interpret the viability scan immediately after the scan and discuss with the interventionalist to perform revascularization based on the integrated information of ICA and viability imaging. This whole process can be completed within 20 minutes, and coronary revascularization can be performed immediately, eliminating, in part, any unnecessary time delay between ICA and intervention and the potential hazard from additional contrast agent use of MSCT or cardiac MRI. Forthcoming studies are needed to fully address the clinical utility, safety, and efficacy of this novel protocol.

5. Limitations

The present study only included subacute (2 weeks) experimentally produced infarcts in swine models. Thus, the feasibility of the current imaging acquisition protocol in an emergency coronary intervention or chronic myocardial infarction setting (ie, >2 weeks) remains to be determined. In addition, the present study was performed using reopened arteries at the time of contrast injection and MSCT image acquisition. In the clinical myocardial infarction setting, the artery may be closed at the time of contrast injection, and the enhancement quality and timing may differ. Forthcoming studies aimed at exploring the contrast kinetics and delayed-enhancement qualities in obstructed arteries appear necessary. Finally, given the design and nature of the present study protocol, myocardial viability

imaging could not be acquired between 0 and 2 minutes after administration of the contrast agent. Additional studies investigating the wash-in and wash-out kinetics of intracoronary contrast administration are required.

6. Conclusion

In the current investigation, the feasibility of myocardial viability assessment by DHE using MSCT after conventional ICA was proven in an experimental swine model. Forthcoming studies are now warranted to address the safety, utility, and validity of concurrent ICA and MSCT within the clinical setting.

Acknowledgments

The content is solely the responsibility of the authors and does not necessarily represent the official views of the National Institutes of Health.

Support: Research reported in this publication was supported by the National Heart, Lung, and Blood Institute, National Institutes of Health (Bethesda, Maryland) under award number R01 HL115150. This work was supported by the IT R&D program of MSIP/KEIT (10044910, Development of Multimodality Imaging and 3D Simulation-Based Integrative Diagnosis-Treatment Support Software System for Cardiovascular Diseases). This study was also funded, in part, by a generous gift from the Dalio Institute of Cardiovascular Imaging (New York, NY) and the Michael Wolk Foundation (New York, NY).

REFERENCES

1. Chareonthaitawee P, Gersh BJ, Araoz PA, Gibbons RJ. Revascularization in severe left ventricular dysfunction: the role of viability testing. *J Am Coll Cardiol.* 2005; 46:567–574. [PubMed: 16098417]
2. Shah BN, Khattar RS, Senior R. The hibernating myocardium: current concepts, diagnostic dilemmas, and clinical challenges in the post-STICH era. *Eur Heart J.* 2013; 34:1323–1336. [PubMed: 23420867]
3. Gerber BL, Rousseau MF, Ahn SA, et al. Prognostic value of myocardial viability by delayed-enhanced magnetic resonance in patients with coronary artery disease and low ejection fraction: impact of revascularization therapy. *J Am Coll Cardiol.* 2012; 59:825–835. [PubMed: 22361403]
4. Knuesel PR, Nanz D, Wyss C, et al. Characterization of dysfunctional myocardium by positron emission tomography and magnetic resonance: relation to functional outcome after revascularization. *Circulation.* 2003; 108:1095–1100. [PubMed: 12939229]
5. Schinkel AF, Bax JJ, Poldermans D, Elhendy A, Ferrari R, Rahimtoola SH. Hibernating myocardium: diagnosis and patient outcomes. *Curr Probl Cardiol.* 2007; 32:375–410. [PubMed: 17560992]
6. Allman KC, Shaw LJ, Hachamovitch R, Udelson JE. Myocardial viability testing and impact of revascularization on prognosis in patients with coronary artery disease and left ventricular dysfunction: a meta-analysis. *J Am Coll Cardiol.* 2002; 39:1151–1158. [PubMed: 11923039]
7. Allman KC. Noninvasive assessment myocardial viability: current status and future directions. *J Nucl Cardiol.* 2013; 20:618–637. quiz 638–619. [PubMed: 23771636]
8. Nandalur KR, Dwamena BA, Choudhri AF, Nandalur MR, Carlos RC. Diagnostic performance of stress cardiac magnetic resonance imaging in the detection of coronary artery disease: a meta-analysis. *J Am Coll Cardiol.* 2007; 50:1343–1353. [PubMed: 17903634]
9. Kim RJ, Fieno DS, Parrish TB, et al. Relationship of MRI delayed contrast enhancement to irreversible injury, infarct age, and contractile function. *Circulation.* 1999; 100:1992–2002. [PubMed: 10556226]
10. Kim RJ, Wu E, Rafael A, et al. The use of contrast-enhanced magnetic resonance imaging to identify reversible myocardial dysfunction. *N Engl J Med.* 2000; 343:1445–1453. [PubMed: 11078769]

11. Schwitter J, Wacker CM, Wilke N, et al. Investigators M-I. Superior diagnostic performance of perfusion-cardiovascular magnetic resonance versus SPECT to detect coronary artery disease: the secondary endpoints of the multicenter multivendor MR-IMPACT II (Magnetic Resonance Imaging for Myocardial Perfusion Assessment in Coronary Artery Disease Trial). *J Cardiovasc Magn Reson*. 2012; 14:61. [PubMed: 22938651]
12. Klein C, Schmal TR, Nekolla SG, Schnackenburg B, Fleck E, Nagel E. Mechanism of late gadolinium enhancement in patients with acute myocardial infarction. *J Cardiovasc Magn Reson*. 2007; 9:653–658. [PubMed: 17578720]
13. Lardo AC, Cordeiro MA, Silva C, et al. Contrast-enhanced multidetector computed tomography viability imaging after myocardial infarction: characterization of myocyte death, microvascular obstruction, and chronic scar. *Circulation*. 2006; 113:394–404. [PubMed: 16432071]
14. Shapiro MD, Sarwar A, Nieman K, Nasir K, Brady TJ, Cury RC. Cardiac computed tomography for prediction of myocardial viability after reperfused acute myocardial infarction. *J Cardiovasc Comput Tomogr*. 2010; 4:267–273. [PubMed: 20580906]
15. Thilo C, Hanley M, Bastarrika G, Ruzsics B, Schoepf UJ. Integrative computed tomographic imaging of cardiac structure, function, perfusion, and viability. *Cardiol Rev*. 2010; 18:219–229. [PubMed: 20699669]
16. Broome DR, Girguis MS, Baron PW, Cottrell AC, Kjellin I, Kirk GA. Gadodiamide-associated nephrogenic systemic fibrosis: why radiologists should be concerned. *AJR Am J Roentgenol*. 2007; 188:586–592. [PubMed: 17242272]
17. Sato A, Nozato T, Hikita H, et al. Prognostic value of myocardial contrast delayed enhancement with 64-slice multidetector computed tomography after acute myocardial infarction. *J Am Coll Cardiol*. 2012; 59:730–738. [PubMed: 22340265]
18. Clark JD, Gebhart GF, Gonder JC, Keeling ME, Kohn DF. The 1996 guide for the care and use of laboratory animals. *ILAR J*. 1997; 38:41–48. [PubMed: 11528046]
19. Mahnken AH, Jost G, Bruners P, et al. Multidetector computed tomography (MDCT) evaluation of myocardial viability: intraindividual comparison of monomeric vs. dimeric contrast media in a rabbit model. *Eur Radiol*. 2009; 19:290–297. [PubMed: 18751712]
20. Buecker A, Katoh M, Krombach GA, et al. A feasibility study of contrast enhancement of acute myocardial infarction in multislice computed tomography: comparison with magnetic resonance imaging and gross morphology in pigs. *Invest Radiol*. 2005; 40:700–704. [PubMed: 16230902]
21. Baks T, Cademartiri F, Moelker AD, et al. Multislice computed tomography and magnetic resonance imaging for the assessment of reperfused acute myocardial infarction. *J Am Coll Cardiol*. 2006; 48:144–152. [PubMed: 16814660]
22. Raff GL, Abidov A, Achenbach S, et al. Society of Cardiovascular Computed Tomography. SCCT guidelines for the interpretation and reporting of coronary computed tomographic angiography. *J Cardiovasc Comput Tomogr*. 2009; 3:122–136. [PubMed: 19272853]
23. McGraw KO, Wong SP. Forming inferences about some intraclass correlation coefficients. *Psychol Methods*. 1996; 1:30–46.
24. Inaba Y, Chen JA, Bergmann SR. Quantity of viable myocardium required to improve survival with revascularization in patients with ischemic cardiomyopathy: a meta-analysis. *J Nucl Cardiol*. 2010; 17:646–654. [PubMed: 20379861]
25. D'Egidio G, Nichol G, Williams KA, et al. Investigators P- Increasing benefit from revascularization is associated with increasing amounts of myocardial hibernation: a substudy of the PARR-2 trial. *JACC Cardiovasc Imaging*. 2009; 2:1060–1068. [PubMed: 19761983]
26. Patel MR, White RD, Abbara S, et al. American College of Radiology Appropriateness Criteria C, American College of Cardiology Foundation Appropriate Use Criteria Task Force. 2013 ACCF/ACR/ASE/ASNC/SCCT/SCMR appropriate utilization of cardiovascular imaging in heart failure: a joint report of the American College of Radiology Appropriateness Criteria Committee and the American College of Cardiology Foundation Appropriate Use Criteria Task Force. *J Am Coll Cardiol*. 2013; 61:2207–2231. [PubMed: 23500216]
27. Beanlands RS, Nichol G, Huszti E, et al. Investigators P- F-18-fluorodeoxyglucose positron emission tomography imaging-assisted management of patients with severe left ventricular

- dysfunction and suspected coronary disease: a randomized, controlled trial (PARR-2). *J Am Coll Cardiol.* 2007; 50:2002–2012. [PubMed: 17996568]
28. Gerber BL, Belge B, Legros GJ, et al. Characterization of acute and chronic myocardial infarcts by multidetector computed tomography: comparison with contrast-enhanced magnetic resonance. *Circulation.* 2006; 113:823–833. [PubMed: 16461822]
 29. Baks T, Cademartiri F, Moelker AD, et al. Assessment of acute reperfused myocardial infarction with delayed enhancement 64-MDCT. *AJR Am J Roentgenol.* 2007; 188:W135–137. [PubMed: 17242218]
 30. Deseive S, Bauer RW, Lehmann R, et al. Dual-energy computed tomography for the detection of late enhancement in reperfused chronic infarction: a comparison to magnetic resonance imaging and histopathology in a porcine model. *Invest Radiol.* 2011; 46:450–456. [PubMed: 21427592]

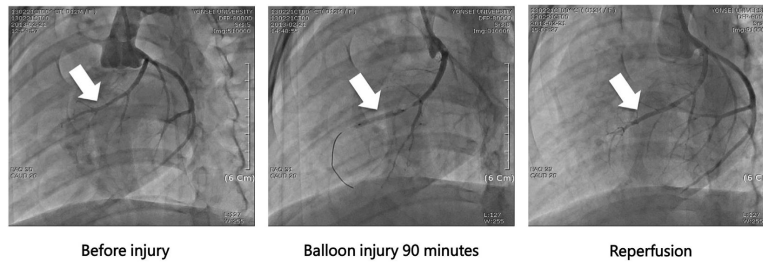


Fig. 1. Representative invasive coronary angiography images acquired before, during, and after balloon injury (white arrow) for creation of myocardial infarction.

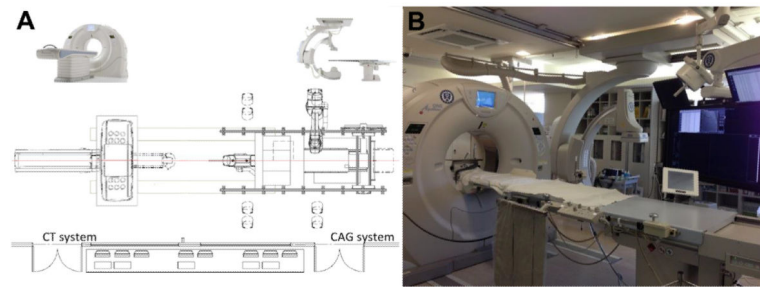


Fig. 2. Schematic illustration (A) and actual image (B) of a novel cardiovascular interventional therapeutic CT system for a consecutive acquisition of invasive coronary angiography and myocardial viability imaging by multislice CT.

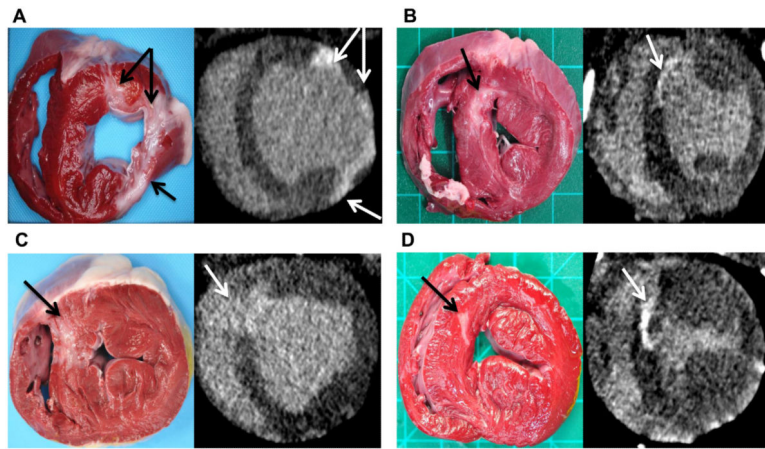


Fig. 3. Examples of comparisons of histopathologic specimens and multislice CT images on the 4 swine models (A-D). The black and white arrows indicate TTC-stained area on histopathologic specimen and hyperenhanced regions on MSCT respectively.

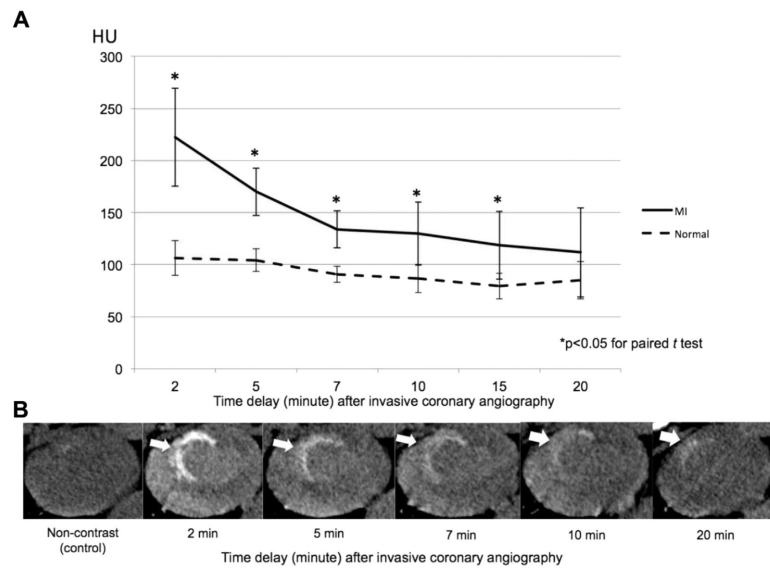


Fig. 4. Time course of CT attenuation (Hounsfield unit [HU]) (A) in myocardial infarct (MI) tissue and remote normal myocardium (normal) and example of short-axis images (B) after intracoronary injection of iodine contrast for conventional invasive coronary angiography.

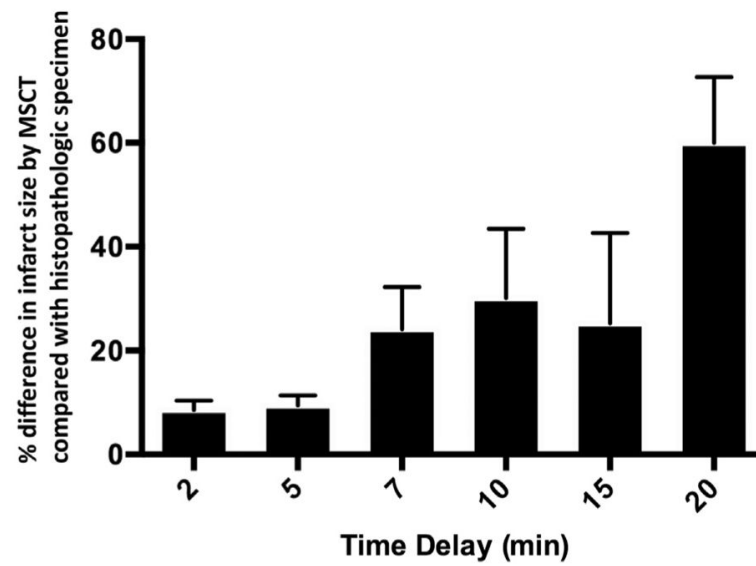


Fig. 5. The percentage difference in infarct size by multislice CT (MSCT) compared with histopathologic specimen at each time point after intracoronary contrast injection for conventional invasive coronary angiography.

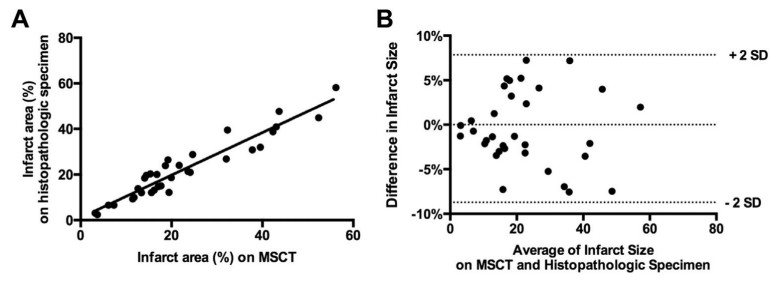


Fig. 6. The correlation (A) and Bland-Altman analyses (B) of infarct sizes assessed by histopathologic specimen and multislice CT (MSCT).

Author Manuscript

Author Manuscript

Author Manuscript

Author Manuscript

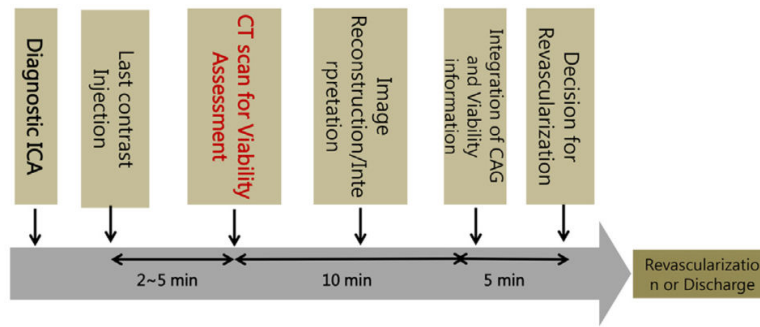


Fig. 7. Conceptual framework of viability assessment using a cardiovascular interventional therapeutic CT system in a patient with suspected coronary artery disease and severe left ventricular dysfunction. ICA, invasive coronary angiography.